J Mol Model (2008) 14:833–841
DOI 10.1007/s00894-008-0311-2

ORIGINAL PAPER

Toward the virtual screening of Cdc25A phosphatase inhibitors with the homology modeled protein structure

Hwangseo Park · Young Ho Jeon

Received: 22 November 2007 / Accepted: 4 April 2008 / Published online: 27 May 2008

Abstract Cdc25 phosphatases have been considered as attractive drug targets for anticancer therapy due to the correlation of their overexpression with a wide variety of cancers. As a method for the discovery of novel inhibitors of Cdc25 phosphatases, we have evaluated the computer-aided drug design protocol involving the homology modeling of Cdc25A and virtual screening with the two docking tools: FlexX and the modified AutoDock program implementing the effects of ligand solvation in the scoring function. The homology modeling with the X-ray crystal structure of Cdc25B as a template provides a high-quality structure of Cdc25A that enables the structure-based inhibitor design. Of the two docking programs under consideration, AutoDock is found to be more accurate than FlexX in terms of scoring putative ligands. A detailed binding mode analysis of the known inhibitors shows that they can be stabilized in the active site of Cdc25A through the simultaneous establishment of the multiple hydrogen bonds and the hydrophobic interactions. The present study demonstrates the usefulness of the modified AutoDock program as a docking tool for virtual screening of new Cdc25 phosphatase inhibitors as well as for binding mode analysis to elucidate the activities of known inhibitors.

H. Park (✉)
Department of Bioscience and Biotechnology, Sejong University,
98 Kunja-Dong, Kwangjin-Ku,
Seoul 143-747, Korea
e-mail: hspark@sejong.ac.kr

Y. H. Jeon (✉)
The Magnetic Resonance Team, Korea Basic Science Institute,
804-1 Yangchung-Ri, Ochang,
Chungbuk 363-883, Korea
e-mail: yhjeon@kbsi.re.kr

Keywords Cdc25A · Docking · Homology modeling · Scoring function · Virtual screening

Introduction

Cdc25 phosphatases belong to a class of dual-specificity phosphatases that are responsible for dephosphorylating both threonine and tyrosine side chains of a protein substrate. Of the three Cdc25 homologues (Cdc25A, Cdc25B, and Cdc25C) encoded in the human genome, Cdc25A and Cdc25B are shown to have oncogenic properties [1]. Cdc25A participates in the control of both G_1-to-S and G_2-to-M transitions in cell cycle by dephosphorylating and activating cyclin-dependent kinase (Cdk)/cyclin complexes, while Cdc25B is mainly involved in regulating the progression at the G_2-to-M transition [2]. Thus, Cdc25 phosphatases play a significant role in the regulation of the eukaryotic cell cycle progression by activating the Cdk/cyclins that serve as the central regulators of the cell cycle with the role of driving each state of cell division.

Due to such an important contribution to the cell cycle regulation, Cdc25 phosphatases have been considered to be involved in oncogenic transformations and human cancers. The overexpression of Cdc25A and Cdc25B has been observed in a variety of tumor cells including breast cancer [3], colon cancer [4, 5], non-Hodgkin's lymphoma [6], prostate cancer [7], pancreatic ductal adenocarcinoma [8], and lung cancer [9, 10]. Recent studies have also shown the involvement of Cdc25A in the adhesion-dependent proliferation of acute myeloid leukaemia (AML) cells [11]. Further evidence for the oncogenic property of Cdc25 phosphatases was provided by the pharmacological studies in which the treatment of Cdc25 phosphatase inhibitors

retarded the growth of the cancer cell lines expressing a high level of Cdc25 phosphatases [12]. It is now most likely that the overexpression of either Cdc25A or Cdc25B leads to the promotion of cell cycle progression in cancer cells although a simultaneous overexpression of both homologues was also observed in more aggressive cancers [13]. Thus, the inhibition of the Cdc25 phosphatases may represent a novel therapeutic approach for the development of anticancer therapeutics although more details about the involvement of Cdc25A and Cdc25B overexpression in tumorigenesis remain to be clarified.

Structural investigations of Cdc25 phosphatases have lagged behind the mechanistic and pharmacological studies. So far several X-ray crystal structures of the catalytic domains of Cdc25A and Cdc25B have been reported in their ligand-free forms only [14, 15]. The lack of structural information about the nature of the interactions between Cdc25 phosphatases and small molecule inhibitors has made it a difficult task to discover good lead compounds for anticancer drugs. The structure-based design of Cdc25 inhibitors has also been hampered by the shallow active site region exposed to bulk solvent as well as the nucleophilic reactivity of the thiolate anion of the catalytic cysteine residue. Nonetheless, a number of effective inhibitors of Cdc25 phosphatases have been discovered with structural diversity as recently reviewed in a comprehensive manner [16–18]. Most of the Cdc25 inhibitors reported in the literature have stemmed from either the isolation of new scaffolds by high throughput screening [19] or the generation of the improved derivatives of pre-existing inhibitor scaffolds [20–24]. Binding modes of the newly found Cdc25 inhibitors have also been investigated with docking simulations in the active site of Cdc25B to gain structural insight into their inhibitory mechanism [25–27]. Cdc25A has been excluded in these docking analyses, because its active site revealed in the existing X-ray structure is flatter and more exposed to bulk solvent than that of Cdc25B. This indicates the necessity of another protein conformation for a structure-based design of Cdc25 phosphatase inhibitors with Cdc25A as the target protein.

In the present study, we address the applicability of a computer-aided drug design protocol involving the homology modeling of Cdc25A and the structure-based virtual screening with docking simulations as a tool for identifying novel classes of potent Cdc25 phosphatase inhibitors. Cdc25A is selected as the target protein in virtual screening instead of Cdc25B because the former has not been considered in the previous docking studies. Therefore, the use of Cdc25A would reduce the possibility of discovering the known inhibitors in a redundant manner. The X-ray structure of Cdc25B was used as the template for the homology modeling of Cdc25A because it possesses a binding pocket around the active site that can accommodate a putative inhibitor. The characteristic feature that discriminates our virtual screening approach from the others lies in the implementation of an accurate solvation model in calculating the binding free energy between Cdc25A and its putative inhibitors, which would have the effect of enhancing the hit rate in enzyme assay [28, 29]. To the best of our knowledge, we report the first example for the usefulness of the structure-based virtual screening of Cdc25 phosphatase inhibitors. It will be shown that the docking simulation with the improved scoring function can be a valuable tool for enriching the chemical library with the molecules that are likely to have a desired biological activity.

Computational methods

Homology modeling of Cdc25A

Although the X-ray crystal structure of Cdc25A has been reported in a ligand-free form [14], it is inappropriate to be used in docking simulation of putative inhibitors because the active site region is maintained flat and exposed to bulk solvent. In order to obatin another conformation of Cdc25A suitable for structure-based virtual screening, therefore, we carried out the homology modeling using the X-ray structure of Cdc25B (PDB ID: 1cws) as a template. This homology modeling started with the retrieval of the peptide sequence of human Cdc25A comprising 524 amino acid residues from the SWISS-PROT protein sequence data bank (http://www.expasy.org/sprot/; accession number P30304) [30]. Sequence alignment between the catalytic domains of Cdc25A and Cdc25B was then derived with the ClustalW package [31] using the BLOSUM matrices for scoring the alignments. The parameters of GAP OPEN, GAP EXTENTION, and GAP DISTANCE were set equal to 10, 0.05, 8, respectively. Opening and extension gap penalties were thus changed systematically, and the obtained alignment was inspected for violation of structural integrity in the structurally conserved regions. Based on the best-scored sequence alignment, the three dimensional structure of the catalytic domain of Cdc25A was constructed using the MODELLER 6v2 program [32]. In this model building, we employed an optimization method involving conjugate gradients and molecular dynamics to minimize the violations of the spatial restraints. With respect to the structure of gap regions, the coordinates were built from a randomized distorted structure that is located approximately between the two anchoring regions as implemented in MODELLER 6v2. To increase the accuracy of calculated structure, the loop modeling was also performed with the enumeration algorithm [33]. Then,

we calculated the conformational energy of the predicted structure of Cdc25A with ProSa 2003 program [34] for the purpose of evaluation.

Constructions of a docking library

The docking library for Cdc25A comprises its own 20 known inhibitors in addition to the 980 compounds selected from the MDL Drug Data Report (MDDR) database. This selection was based on drug-like filters that adopt only the compounds with physicochemical properties of potential drug candidates [35] and without reactive functional group (s). On the basis of "Rule of five", we selected only the compounds with the molecular weights less than 500, cLogP values between −5 and 5, the number of hydrogen bond donors less than 5, the number of hydrogen bond acceptors less than 10, and the number of rotatable bonds less than 10. All of the compounds included in the docking library were then subjected to the Corina32 program to generate their 3-D coordinates, which was followed by the assignment of Gasteiger-Marsilli atomic charges [36]. In the conversion of molecular coordinates, one single stereoisomer was generated and the compounds with carboxylic acid group(s) were assumed to be deprotonated. The chemical structures of the 20 known inhibitors of Cdc25A seeded in the docking library are shown in Appendices.

Virtual screening of Cdc25A inhibitors with AutoDock

We used the automated version of the AutoDock3.0.5 program [37] because the outperformance of its scoring function over those of the others had been demonstrated for several target proteins [38]. The atomic coordinates of Cdc25A obtained from the homology modeling were used as the receptor model in the virtual screening with docking simulations. A special attention was paid to assign the protonation states of the ionizable Asp, Glu, His, and Lys residues. The side chains of Asp and Glu residues were assumed to be neutral if one of their carboxylate oxygens pointed toward a hydrogen-bond accepting group including the backbone aminocarbonyl oxygen at a distance within 3.5 Å, a generally accepted distance limit for a hydrogen bond of moderate strength [39]. Similarly, the lysine side chains were protonated unless the NZ atom was in proximity of a hydrogen-bond donating group. The same procedure was also applied to determine the protonation states of ND and NE atoms in His residues. The catalytic cysteine residue (Cys430) of Cdc25A was assumed to be deprotonated.

In the actual docking simulation of the compounds in the docking library, we used the empirical AutoDock scoring function improved with a new solvation model for a compound. The modified scoring function has the following form:

$$\begin{aligned}\Delta G_{bind}^{aq} = {} & W_{vdW}\sum_{i=1}\sum_{j>i}\left(\frac{A_{ij}}{r_{ij}^{12}}-\frac{B_{ij}}{r_{ij}^{6}}\right) \\ & + W_{hbond}\sum_{i=1}\sum_{j>i}E(t)\left(\frac{C_{ij}}{r_{ij}^{12}}-\frac{D_{ij}}{r_{ij}^{10}}\right) \\ & + W_{elec}\sum_{i=1}\sum_{j>i}\frac{q_i q_j}{\varepsilon(r_{ij})r_{ij}} + W_{tor}N_{tor} \\ & + W_{sol}\sum_{i=1}S_i\left(Occ_i^{\max}-\sum_{j>i}V_j e^{-\frac{r_{ij}^2}{2\sigma^2}}\right) \qquad (1)\end{aligned}$$

where W_{vdW}, W_{hbond}, W_{elec}, W_{tor}, and W_{sol} are weighting factors of van der Waals, hydrogen bond, electrostatic interactions, torsional term, and desolvation energy of inhibitors, respectively. r_{ij} represents the interatomic distance, and A_{ij}, B_{ij}, C_{ij}, and D_{ij} are related to the depths of energy well and the equilibrium separations between the two atoms. The hydrogen bond term has an additional weighting factor, $E(t)$, representing the angle-dependent directionality. With respect to the distant-dependent dielectric constant, $\varepsilon(r_{ij})$, a sigmoidal function proposed by Mehler et al. [40] was used in computing the interatomic electrostatic interactions between the receptor protein and its putative ligands. In the entropic term, N_{tor} is the number of the rotatable bonds in a ligand. In the desolvation term, S_i and V_i are the solvation parameter and the fragmental volume of atom i [41], respectively, while $Occ_i^{\max}$ stands for the maximum atomic occupancy. In the calculation of molecular solvation free energy term in Eq. (1), we used the atomic parameters recently developed by Kang et al. [42] because those of the atoms other than carbon were unavailable in the current version of AutoDock. This modification of the solvation free energy term is expected to increase the accuracy in virtual screening, because the underestimation of ligand solvation often leads to the overestimation of the binding affinity of a ligand with many polar atoms [29].

The docking simulation of a compound in the docking library started with the calculation the 3-D grids of interaction energy for all of the possible atom types present in chemical database. These uniquely defined potential grids for the receptor protein were then used in common for docking simulations of all compounds in the docking library. As the center of the common grids in the active site, we used the center of mass coordinates of the docked structure of the probe molecule, NSC 95397, whose binding mode in the active site of Cdc25B had been well characterized in the previous docking simulations [27]. The calculated grid maps were of dimension 61×61×61 points with the spacing of 0.375 Å, yielding a receptor model that

includes atoms within 22.9 Å of the grid center. For each compound in the docking library, 10 docking runs were performed with the initial population of 50 individuals. Maximum number of generations and energy evaluation were set to 27,000 and 2.5×10^5, respectively. Docking simulations with AutoDock were then carried out in the active site of Cdc25A to score and rank the compounds in the docking library according to the binding affinity for Cdc25A.

Virtual screening of Cdc25A inhibitors with FlexX

All default parameters, as implemented in Sybyl 6.9, were used for the target protein and all compounds in the docking library. The active site and the interaction surface of the receptor were defined by using the reference ligand, NSC 95397, whose binding mode had been calculated with docking simulations and cutoff distance of 6.5 Å. The conformational flexibility of a ligand was modeled by a discrete set of preferred torsional angles for acyclic single bonds. Base fragments were then selected automatically with the maximum number of four. A base fragment was placed into the active site based on the two algorithms. The first one superimposes triples of interaction centers of the base fragment with triples of compatible interaction sites. Second, the matching algorithm was used when the base fragment had fewer than three interaction centers. The empirical scoring function given in Eq. (2) was used for ranking the binding modes of each ligand in the prepared docking library [43]:

$$\begin{aligned}\Delta G_{bind} = \Delta G_0 &+ W_{hbond}\sum_{hbonds} f(\Delta R,\Delta\alpha) \\ &+ W_{ionic}\sum_{ionic} f(\Delta R,\Delta\alpha) \\ &+ W_{aro/aro}\sum_{aro/aro} f(\Delta R,\Delta\alpha) \\ &+ W_{lipo}\sum_{lipo} f^{*}(\Delta R) + W_{tor}N_{tor}\end{aligned} \quad (2)$$

Here, $f(\Delta R\Delta\alpha)$ is a scaling function penalizing the deviations from the ideal distances and angles and $f^*(\Delta R)$ penalizes the forbiddingly close contacts between lipophilic interactions involving nonaromatic groups.

Results and discussion

Homology modeling of Cdc25A

Figure 1 displays the sequence alignment of the catalytic domains of Cdc25A and Cdc25B, which were used as the target and the template for homology modeling, respectively. We note that the result of sequence alignment is the same as that obtained by Reynolds et al. [15]. According to this alignment, the sequence identity and the similarity amount to 66.7% and 83.0%, respectively. Judging from such a high sequence homology, a high-quality 3D structure of Cdc25A can be obtained in the homology modeling. It is indeed well known that the homology-modeled structure of a target protein can be accurate enough to be used in the structure-based ligand design as well as in the study of catalytic mechanism once the sequence identity between target and template exceeds 60% [44]. Based on the sequence alignment shown in Fig. 1, ten structural models of Cdc25A were calculated and the one with the lowest value of MODELLER objective function was selected as the final model of Cdc25A to be used in the subsequent virtual screening with docking simulations.

Figure 2 shows the structure of Cdc25A obtained from the homology modeling in comparison to the X-ray structure of Cdc25B that was used as the template. As expected from the high sequence identity, the target and the template possess a very similar folding structure and are superimposable over the main chain atoms. Despite the overall structural similarity, however, two different structural features are observed around the active site. We first note that the residue Met403 near the active site of Cdc25A differs from the corresponding Leu445 in Cdc25B. As can be seen in Fig. 2, the distances between the former and the neighboring active site residues (Arg436 and Arg501) are shorter than those between the latter and the corresponding Arg479 and Arg544 in the active site of Cdc25B. This difference has an effect of differentiating the accessibility of the active site between the two Cdc25 phosphatases. The second structural difference around the active sites is in the position of the Met residue located at the top of active site. Met488 points toward the cavity of the active site in Cdc25A, whereas the corresponding Met531 is directed outward to bulk solvent in Cdc25B. Due to the two structural differences, the volume of the active site of Cdc25A is smaller than that of Cdc25B. Apparently, such a difference in active site geometry can serve as a clue for designing the selective Cdc25 phosphatase inhibitors.

The final structural model of Cdc25A obtained from the homology modeling was evaluated with the ProSa 2003 program by examining whether the interaction of each residue with the remainder of the protein is maintained favorable. This program calculates the knowledge-based mean fields to judge the quality of protein folds, and has been widely used to measure the stability of a protein conformation. Figure 3 shows the ProSa 2003 energy profile of the homology-modeled Cdc25A in comparison to those of the X-ray structures of Cdc25A and Cdc25B. We note that the ProSa energy remains negative for each amino acid residue in all three cases, indicating that all of

```
Cdc25A  332  DPRDLIGDFSKGYLFHTVAGKHQDLKYISPEIMASVLNGKFANLIKEFVIIDCRYPYEYE 391
Cdc25B  374  DHRELIGDYSKAFLLQTVDGKHQDLKYISPETMVALLTGKFSNIVDKFVIVDCRYPYEYE 433

Cdc25A  392  GGHIKGAVNLHMEEEVEDFLLKKPIVPTD-GKRVIVVFHCEFSSERGPRMCRYVRERDRL 450
Cdc25B  434  GGHIKTAVNLPLERDAESFLLKSPIAPCSLDKRVILIFHCEFSSERGPRMCRFIRERDRA 493

Cdc25A  451  GNEYPKLHYPELYVLKGGYKEFFMKCQSYCEPPSYRPMHHEDFKEDLKKFRTKSRTW    507
Cdc25B  494  VNDYPSLYYPEMYILKGGYKEFFPQHPNFCEPQDYRPMNHEAFKDELKTFRLKTRSW    550
```

Fig. 1 Sequence alignment of the catalytic domains of Cdc25A and Cdc25B. The identity and the similarity between the corresponding residues are indicated in red and green, respectively. The residues constituting the active site are indicated in dotted rectangular box

the three protein structures should be acceptable. More interestingly, the homology-modeled structure of Cdc25A reveals a higher stability than the X-ray structure in most part of the protein. This supports the possibility that the homology modeling with a high sequence identity and a high-quality template structure can produce a 3-D structure of a target protein comparable in accuracy to the X-ray crystal structure [44].

As a further evaluation of the homology-modeled structure of CDC25A, the final model obtained with MODELLER was subject to stereochemical analysis with the PROCHECK program. The results show that the backbone Φ and Ψ dihedral angles of 72.7%, 24.4%, and 2.8% of the residues are located within most favorable, additionally allowed, and generously allowed regions of the Ramachandran plot, respectively, with no residue in disallowed region. This good stereochemical quality is not surprising for the high sequence identity (66.7%) and similarity (83.0%) between the template and the target as illustrated in Fig. 1.

Virtual screening

We have tested the performances of the automated AutoDock and FlexX in the virtual screening of Cdc25A inhibitors. This comparative evaluation was done with the homology-modeled structure of Cdc25A as the target protein and the docking library that contains 980 randomly chosen drug-like molecules and 20 known inhibitors. Compared in Fig. 4 are the percentages of true hits retrieved by the AutoDock and FlexX in increasing fractions of the starting database. We note that the AutoDock performs better than FlexX in providing the highest enrichment at every fraction cutoff. It picks five actives seeded in top 1% of the database as compared to one for FlexX. The performance of AutoDock becomes clearer when one compares the ability to pick out the most actives out of a cumulative total of 20 used in this study. When 10% of the database is considered, for example, the AutoDock retrieved a total of 12 actives out of the total 20 known inhibitors, contrary to four actives by FlexX. Thus, the outperformance of the automated AutoDock reveals a consistency for all cutoffs, indicating that it can be a promising docking tool for virtual screening of Cdc25A inhibitors.

The difference in the accuracies of AutoDock and FlexX in database screening can be understood by comparing their respective scoring functions. It is common to the two docking programs that their scoring functions include the

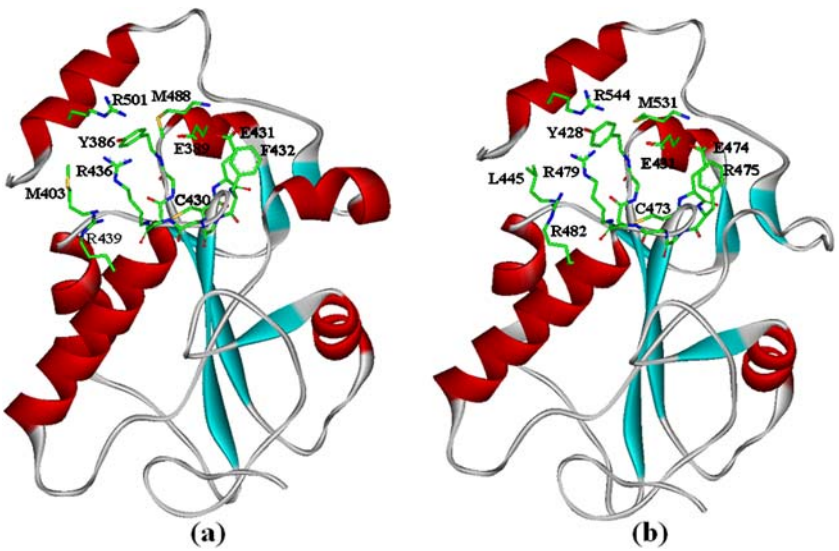

Fig. 2 Comparative view of (**a**) the homology-modeled structure of Cdc25A and (**b**) the X-ray crystal structure of Cdc25B

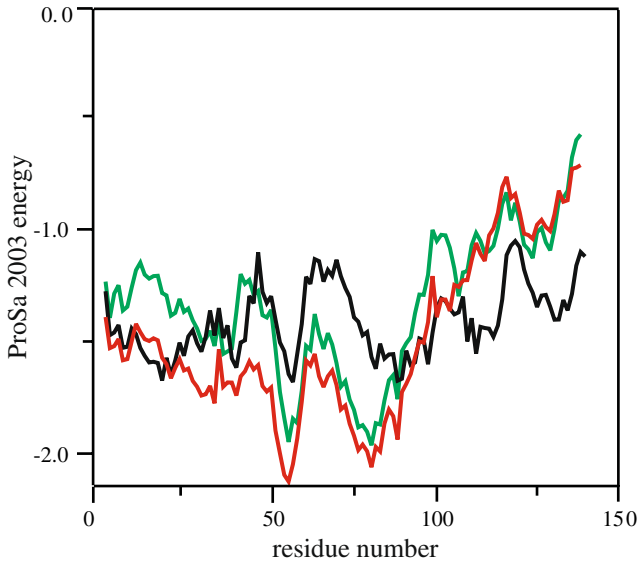

Fig. 3 Comparison of ProSa energy profiles for the homology-modeled structure of Cdc25A (red), and the X-ray structures of Cdc25A (green) and Cdc25B (black). For convenience, the amino acids of both Cdc25 phosphatases are renumbered from 1 instead of retaining their original numbers

angle-dependent directionality of a hydrogen bond and entropic penalty for the formation of a protein-ligand complex. On the other hand, there are two characteristic features that discriminate the scoring function of AutoDock from that of FlexX: the use of a sigmoidal distance-dependent dielectric function in the electrostatic term and desolvation cost for complexation of a ligand in the binding site. The former has an effect of modeling solvent screening in the electrostatic interactions between charged atoms [40]. This is important because the top-scored ligands obtained with a small value of dielectric constant tend to possess many atoms with high partial charges as a consequence of the overestimation of electrostatic interactions. The effect of ligand solvation is also important, particularly in comparing many putative ligands that differ in polarity and size. The hit compounds may have a severe charge separation on their molecular structures or be larger than expected unless the energy of the solvated state is considered in docking simulations [29]. Thus, a significant outperformance of AutoDock over FlexX should be attributed to the inclusion of solvation term in the scoring function as well as a more proper description of electrostatic interactions between protein and ligand atoms.

Molecular modeling studies of the known inhibitors

Virtual screening with AutoDock predicts that the two compounds (1 and 2 in Fig. 5) are the strongest binders in the active site of Cdc25A among the 20 known inhibitors under consideration, the systematic names of which are 3-[4,6-dichloro-7-(3-methyl-but-2-enyl)-1*H*-indol-3-yl]-2,5-dihydroxy-[1, 4]benzoquinone and 1-biphenyl-4-yl-3,4-bis-(2-hydroxy-ethylsulfanyl)-pyrrole-2,5-dione, respectively. We note that both inhibitors possess two carbonyl and two hydroxyl groups, indicating the involvement of multiple hydrogen bonds in their interactions with the active site of Cdc25A. It is also a common structural feature of the two inhibitors that a hydrophobic group is attached at the end of molecular structure. Apparently, such hydrophobic moieties seem to be stabilized at the active site through the interaction with the nonpolar groups of Cdc25A.

To gain more structural insight into the inhibitory mechanism for Cdc25A, the binding modes of 1 and 2 were examined using the AutoDock program with the procedure described in the previous section. Their calculated binding modes of the two inhibitors in the active site of Cdc25A are compared in Fig. 6. We see that both 2,5-dihydroxy-[1, 4] benzoquinone group of 1 and pyrrole-2,5-dione group of 2 reside in the vicinity of the catalytic residue, Cys430, indicating that each of the two moieties may serve as a surrogate for the substrate phosphate group. It is also noted that three hydrogen bonds are established between one carbonyl and two phenolic oxygens of 1 and three backbone aminocarbonyl groups of Cdc25A. Similarly, one carbonyl and two hydroxyl oxygens of 2 form three hydrogen bonds with two backbone amidic nitrogens and a sidechain guanidium group of Arg501. Judging from the presence of the multiple hydrogen bonds in the two binding configurations, the carbonyl and hydroxyl groups of the inhibitors seem to play the role of anchor for binding of the inhibitors in the active site of Cdc25A in a cooperative fashion. The nonpolar moieties of the two inhibitors are stabilized by hydrophobic interactions with the side chains of Met488, Trp507, and Arg residues around the active site.

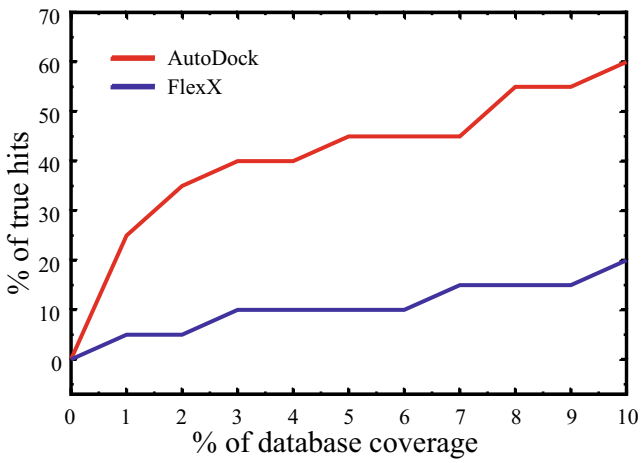

Fig. 4 The cumulative percentage of known Cdc25A inhibitors recovered by virtual screening as a function of the top-scoring fraction of database selected for generating a hit list

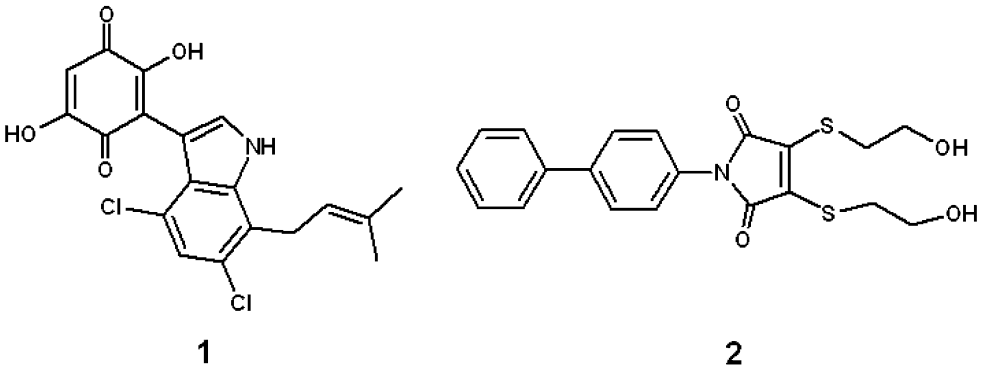

Fig. 5 Chemical structures of the top-scored Cdc25A inhibitors in the virtual screening.

Not only the establishment of multiple hydrogen bonds but also the formation of such hydrophobic contacts seem to be important in stabilizing the inhibitors in the active site of Cdc25A. This is due to the exposure of the active site to bulk solvent, which has an effect of facilitating the diffusive intrusion of solvent molecules into the active site. The hydrophobic contacts between protein and ligand atoms should be less affected than the interactions between polar groups by the solvent molecules that can reduce the strength of inhibitor binding in the active site. Thus, it is most likely that a strong Cdc25A inhibitor should possess the proper chemical groups arranged in such a way that it can be stabilized in the active site through the establishment of the multiple hydrogen bonds and hydrophobic contacts in a simultaneous manner.

The binding modes of 1 and 2 found in this study are similar to that obtained by Park et al. [27] in the sense that the surrogate groups of the inhibitors for the substrate phosphate moiety are stabilized near the catalytic cysteine residue in the active site through the formation of multiple hydrogen bonds. However, it is not the case in the earlier docking results reported by Lazo et al. [25] and those reported by Lavecchia et al. [26] in which the surrogate group was not accommodated in the active site. This different result exemplifies the importance of the selection of proper docking method and scoring function in calculating the binding mode of a Cdc25 phosphatase inhibitor.

Conclusions

As a method for the discovery of novel inhibitors of Cdc25 phosphatases, we have evaluated the computer-aided drug design protocol involving the homology modeling of Cdc25A and the structure-based virtual screening with the two docking tools: FlexX and the automated and improved AutoDock program implementing the effects of ligand solvation in the binding free energy function. The homology modeling of Cdc25A with the X-ray crystal structure of Cdc25B as a template provides a high-quality structure of Cdc25A that enables the structure-based inhibitor design. Of the two docking programs under consideration, AutoDock is more accurate than FlexX in terms of scoring putative ligands to the extent of 5-fold enhancement of hit rate in database screening when 1% of database coverage is used as a cutoff. It is also shown from a detailed binding

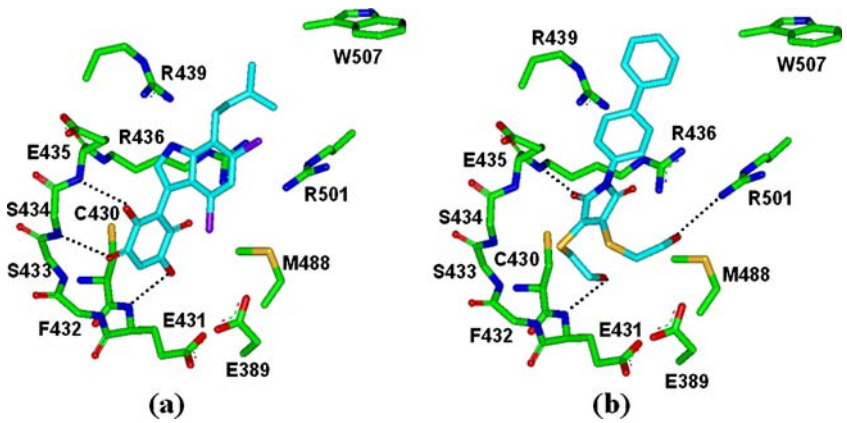

Fig. 6 Calculated binding modes of (**a**) 1 and (**b**) 2 in the active site Cdc25A. Carbon atoms of the protein and the ligand are indicated in green and cyan, respectively. Each dotted line indicates a hydrogen bond

mode analysis of the known inhibitors that their binding in the active site of Cdc25A can be facilitated by the establishment of multiple hydrogen bonds with the backbone and side chain groups. Simultaneously, the hydrophobic interactions with the residues near the active site can also play a significant role in stabilizing the inhibitors in the active site of Cdc25A. These results demonstrate the usefulness of the automated AutoDock program with the improved scoring function as a docking tool for virtual screening of new Cdc25 phosphatase inhibitors as well as for binding mode analysis to elucidate the activities of known inhibitors.

Acknowledgements This work was supported by the Bio-MR Research Program (to Y.H.J., Korea Basic Science Institute) of the Korean Ministry of Science and Technology.

Appendices

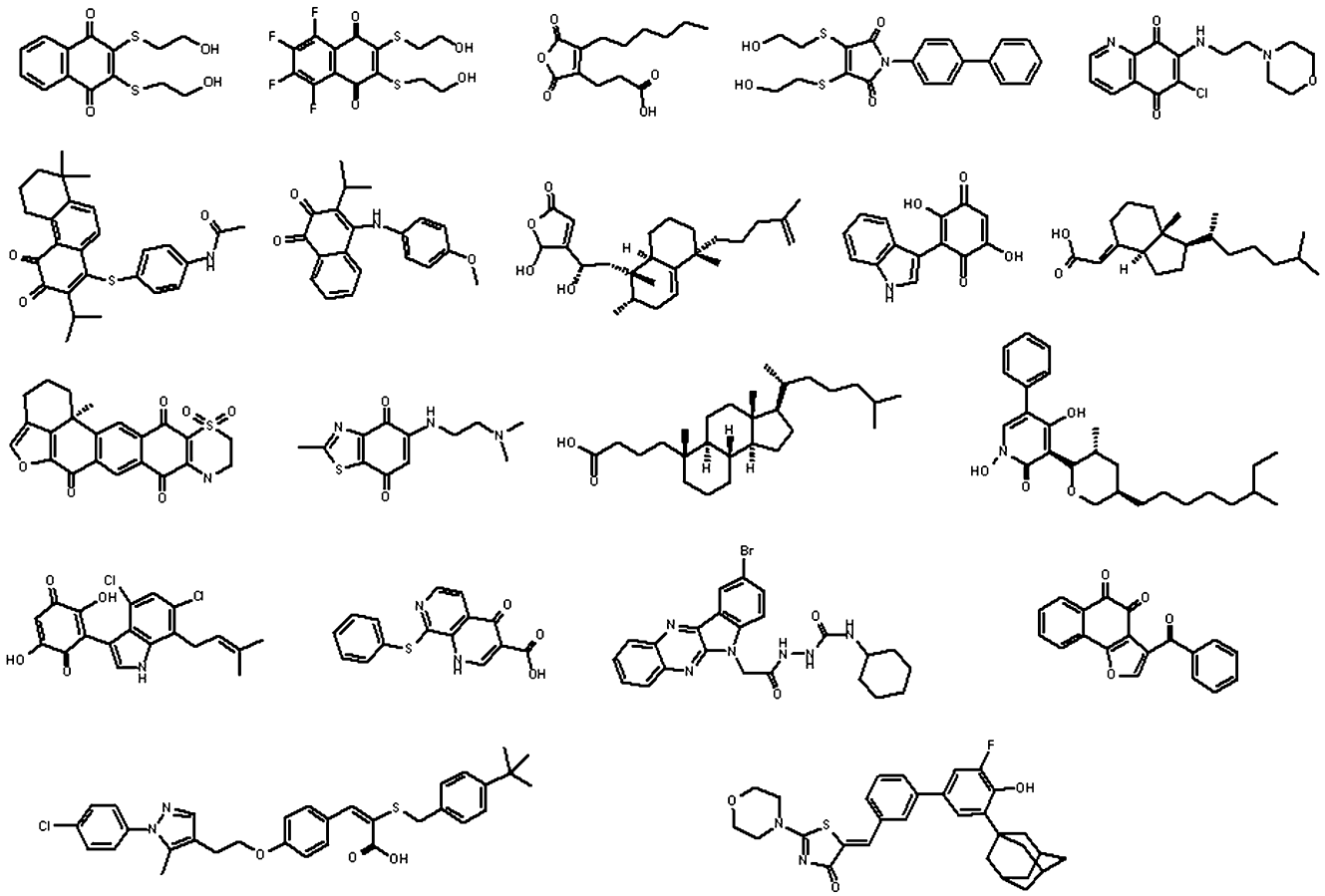

References

1. Kristjansdottir K, Rudolph J (2004) Chem Biol 11:1043–1051
2. Rudolph J (2007) Biochemistry 46:3595–3604
3. Galaktionov K, Lee AK, Eckstein J, Draetta G, Meckler J, Loda M, Beach D (1995) Science 269:1575–1577
4. Hernandez S, Bessa X, Bea S, Hernandez L, Nadal A, Mallofre C, Muntane J, Castells A, Fernandez PL, Cardesa A, Campo E (2001) Lab Invest 81:465–473
5. Takemara I, Yamamoto H, Sekimoto M, Ohue M, Noura S, Miyake Y, Matsumoto T, Aihara T, Tomita N, Tamaki Y, Sakita I, Kikkawa N, Matsuura N, Shiozaki H, Monden M (2000) Cancer Res 60:3043–3050
6. Hernandez S, Hernandez L, Bea S, Pinyol M, Nayach I, Bellosillo B, Nadal A, Ferrer A, Fernandez PL, Montserrat E, Cardesa A, Cardes E, Campo E (2000) Int J Cancer 89:148–152
7. Ngan ESW, Hashimoto Y, Ma X-Q, Tsai MJ, Tsai SY (2003) Oncogene 22:734–739
8. Guo J, Kleeff J, Li J, Ding J, Hammer J, Zhao Y, Giese T, Korc M, Büchler M, Friess H (2004) Oncogene 23:71–81
9. Wu WG, Fan YH, Kemp BL, Walsh G, Mao L (1998) Cancer Res 58:4082–4085
10. Sasaki H, Yukiue H, Kobayashi Y, Tanahashi M, Moriyama S, Nakashima Y, Fukai I, Kiriyama M, Yamakawa Y, Fujii Y (2001) Cancer Lett 173:187–192
11. Fernandez-Vidal A, Ysebaert L, Didier C, Betous R, Toni FD, Prade-Houdellier N, Demur C, Contour-Galcera M-O, Prevost G, Ducommun B, Payrastre B, Racaud-Sultan C, Manenti S (2006) Cancer Res 66:7128–7135
12. Nishikawa Y, Carr BI, Wang M, Kar S, Finn F, Dowd B, Zheng ZB, Kerns J, Naganathan S (1995) J Biol Chem 270:28304–28310
13. Boutros R, Dozier C, Ducommun B (2006) Curr Opin Cell Biol 18:185–191
14. Fauman EB, Cogswell JP, Lovejoy B, Rocque WJ, Holmes W, Montana VG, Piwnica-Worms H, Rink MJ, Saper MA (1996) Cell 93:617–625
15. Reynolds RA, Yem AW, Wolfe CL, Deibel MR, Chidester CG, Watenpaugh KD (1999) J Mol Biol 293:559–568
16. Contour-Galcera M-O, Sidhu A, Prevost G, Bigg D, Ducommun B (2007) Pharmcol Ther 115:1–12
17. Ham SW, Carr BI (2004) Drug Des Rev 1:123–132
18. Prevost G, Brezak M-C, Goubin F, Mondesert O, Galcera M-O, Quaranta M, Alby F, Lavergne O, Ducommun B (2003) Prog Cell Cycle Res 5:225–234
19. Lazo JS, Aslan DC, Southwick EC, Cooley KA, Ducruet AP, Joo B, Vogt A, Wipf P (2001) J Med Chem 44:4042–4049
20. Sohn J, Kiburz B, Li Z, Deng L, Safi A, Pirrung MC, Rudolph J (2003) J Med Chem 46:2580–2588
21. Brault L, Denance M, Banaszak E, Maadidi SE, Battaglia E, Bagrel D, Samadi M (2007) Eur J Med Chem 42:243–247
22. Huang W, Li J, Zhang W, Zhou Y, Xie C, Luo Y, Li Y, Wang J, Li J, Lu W (2006) Bioorg Med Chem Lett 16:1905–1908
23. Brun M-P, Braud E, Angotti D, Mondesert O, Quaranta M, Montes M, Miteva M, Gresh N, Ducommun B, Garbay C (2005) Bioorg Med Chem 13:4871–4879
24. Contour-Galcera M-O, Lavergne O, Brezak M-C, Ducommun B, Prevost G (2004) Bioorg Med Chem Lett 14:5809–5812
25. Lazo JS, Nemoto K, Pestell KE, Cooley K, Southwick EC, Mitchell DA, Furey W, Gussio R, Zaharevitz DW, Joo B, Wipf P (2002) Mol Pharmacol 61:720–728
26. Lavecchia A, Cosconati S, Limongelli V, Novellino E (2006) ChemMedChem 1:540–550
27. Park H, Carr BI, Li M, Ham SW (2007) Bioorg Med Chem Lett 17:2351–2354
28. Zou X, Sun Y, Kuntz ID (1999) J Am Chem Soc 121:8033–8043
29. Shoichet BK, Leach AR, Kuntz ID (1999) Proteins 34:4–16
30. Bairoch A, Apweiler R (1999) Nucl Acids Res 27:49–54
31. Thompson JD, Higgins DG, Gibson TJ (1994) Nucl Acids Res 22:4673–4680
32. Sali A, Blundell TL (1993) J Mol Biol 234:779–815
33. Fiser A, Do RKG, Sali A (2000) Protein Sci 9:1753–1773
34. Sippl MJ (1993) Proteins 17:355–362
35. Lipinski CA, Lombardo F, Dominy BW, Feeney PJ (1997) Adv Drug Delivery Rev 23:3–25
36. Gasteiger J, Marsili M (1980) Tetrahedron 36:3219–3228
37. Morris GM, Goodsell DS, Halliday RS, Huey R, Hart WE, Belew RK, Olson AJ (1998) J Comput Chem 19:1639–1662
38. Park H, Lee J, Lee S (2006) Proteins 65:549–554
39. Jeffrey GA (1997) An introduction to hydrogen bonding. Oxford University Press, Oxford
40. Mehler EL, Solmajer T (1991) Protein Eng 4:903–910
41. Stouten PFW, Frömmel C, Nakamura H, Sander C (1993) Mol Simul 10:97–120
42. Kang H, Choi H, Park H (2007) J Chem Inf Model 47:509–514
43. Böhm HJ (1994) J Comput-Aided Mol Des 8:243–256
44. Baker D, Sali A (2001) Science 294:93–96